Microstructure and Third Order Optical Nonlinearities of Ion-Implanted and Thermally Annealed Cu-SiO_2 Thin Films

Lee Chae, Minyung Lee*, Hyun Kyong Kim†, and Dae Won Moon†

Department of Chemistry, Ewha Womans University, Seoul 120-750, Korea
†Surface Analysis Group, Korea Research Institute for Standards and Science, Taejon 305-606, Korea
Received June 2, 1997

The crystal structure and optical properties of copper nanoparticles, prepared in fused silica by ion-implantation and subsequent heat-treatment, were characterized by X-ray, TEM, linear absorption, and degenerate four-wave mixing (DFWM) technique. The X-ray data show fcc lattice structure of the nanocrystals and their size was measured as 8-20 nanometer by high resolution TEM. Using DFWM, the third-order nonlinear optical coefficient of the Cu-SiO_2 thin films was measured as $0.4\text{-}1.1\times10^{-8}$ esu in the surface plasmon resonance absorption region (540-570 nm).

Introduction

Metal nanoparticles have a potential application in nonlinear optical devices in the future, because it has been frequently reported that metal nanoparticles possess high optical nonlinearity and fast time response in the surface plasmon absorption region.[1-3] Noble metal particles such as Cu, Ag, and Au embedded in glass show the surface plasmon absorption in the ultraviolet to visible.[4-6] Therefore, most intensive optical studies on these materials were carried out in that wavelength region, using linear absorption and nonlinear optical methods.[7-11]

Among three noble metals, optical studies on Cu nanoparticles are relatively rare, due to difficulty in preparation. One of direct methods to obtain metal nanoclusters is to use the high energy ion-implantation method, if available. Magruder *et al.* have first implanted Cu ions in fused silica and observed the formation of nanocrystals.[12] The nanocrystal diameter has been identified as 5-20 nm, depending on the ion dose rate. Yang *et al.* measured the third-order optical nonlinearity of the ion implanted Cu sample using the picosecond degenerate four wave mixing technique (DFWM).[13] They obtained $\chi^{(3)}$ value of 10^{-8}-10^{-9} esu at 532 nm. The sample shows the surface plasmon absorption around 570 nm. Since the interband transition of Cu sample is expected to occur at 590 nm, the observed $\chi^{(3)}$ value is contributed by both mechanism; surface plasmon resonance and interband transition.

In this work, copper nanoparticles were prepared in fused silica by ion-implantation method, which is similar to the method by Magruder *et al.*,[12] but our sample was subsequently heat-treated at high temperature (700 °C). In addition, we closely examine the nanocrystal structure by X-ray scattering and transmission electron microscopy (TEM). The nonlinear optical property was measured by DFWM near the surface plasmon absorption region (540-570 nm). The third order nonlinear optical coefficient, $\chi^{(3)}$, was calculated from the measured data. Finally those values are compared to the reported $\chi^{(3)}$ values of Cu nanocrystal samples prepared by various methods.

Experimental

A quartz plate having $10.0\times10.0\times1.0$ mm dimension was implanted by Cu ions with dose of 6.4×10^{16} ions/cm^2 at an energy of 100 keV. The sample was subsequently heat-treated to 700 °C. The X-ray diffraction data were obtained by Co K_α (1.790 Å). The sample thickness and nanocrystal size were obtained by a high resolution TEM (Hitachi model H-9000). Optical nonlinear measurements were performed using the degenerate four wave mixing experiment with two beam configuration. The laser system was a Coumarin 540 dye laser pumped by a nanosecond Q-switched Nd:YAG laser (Spectra-Physics model 150), producing *ca.* 10 mJ pulse energy at 10 Hz.[11] The bandwidth from the dye laser is reportedly 0.15 cm^{-1}. To avoid sample damage, the laser pulse energy is attenuated, equally split out, and recombined on the sample spatially and temporally for DFWM experiment. The diffracted signal was detected by a photodiode or PMT and was processed in a boxcar.

Results and Discussion

Absorption spectra of Cu nanocrystals. Figure 1 shows the absorption spectrum of Cu ion-implanted nanocrystal sample. The absorption spectra of the sample heat-treated at 300 °C and 700 °C are also shown. Before heat-treatment, the maximum of surface plasmon peak occurs at 560 nm. The heat-treatment shifts the surface plasmon maximum to the red wavelength region, so the sample heat-treated at 700 °C shows the peak 575 nm. In addition to the peak shift, the increase of heating temperature also increases the absorbance. The absorption spectrum heat-treated at 700 °C shows an additional shallow and broad peak around 450-500 nm. Since this spectral range is far off from the surface plasmon absorption region of interest in this study, further identification was not made. Assuming the particles are spherical in shape and the size distribution is narrow enough, the particle's mean diameter is approximately given by the following formula[14]

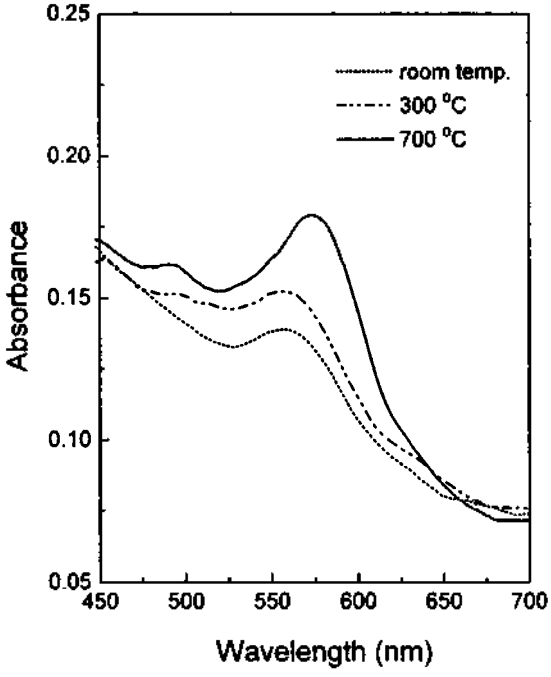

Figure 1. Absorption spectra of Cu-SiO_2 thin film samples at various heat-treatment temperatures.

$$D = 2\frac{V_F}{\Delta\omega^{1/2}} \quad (1)$$

where D is the mean nanocrystal diameter, V_F the Fermi velocity of an electron (1.57×10^8 cm/s for Cu), and $\Delta\omega^{1/2}$ the full width at half maximum of the absorption peak (FWHM). FWHM of the plasmon resonance band was obtained through a Lorentzian fitting with background subtraction for interband transition and the calculated values are 8.4 nm for the sample heat-treated at 700 °C.

X-ray diffraction and TEM data of Cu nanocrystals. X-ray crystallography gives direct information on whether or not the sample forms a crystal structure. Figure 2 is the X-ray data of Cu-SiO_2 thin films. The data clearly show two peaks which are characteristic of the fcc lattice structure. Peaks at 2θ=53.2° and 60.1° correspond to (111) and (200) plane, respectively. The lattice parameter, calculated from those angles and two reflection planes was found to be 3.518 ± 0.055 Å on average. The lattice parameter for bulk Cu crystal is 3.615 Å. So the lattice parameter of Cu nanocrystal formed in fused silica has about 0.1 Å smaller than that of bulk Cu.

Figure 3 is the HRTEM data from which the implanted sample thickness has been identified as ca. 140 nm. To characterize nanocrystal size, the TEM picture was obtained with higher magnification and Cu nanocrystal diameter appears to be in the 8-20 nm range. Figure 4, the enlarged figure of a few nanocrystals, shows the shape is approxmately spherical and exhibits an interference pattern which is indicative of crystallinity of the formed Cu particles.

Nonlinear optical properties of Cu nanocrystals. The optical nonlinearity of Cu nanocrystal samples was measured by DFWM with two beam configuration. Cu-SiO_2 thin film samples heat-treated at 700 °C were chosen because it shows the largest surface plasmon absorption. The sample was excited by two beams having wave vectors of k_1 and k_2 with equal intensity. Two beams are s-polarized with respect to the film surface. The diffracted signals due to third-order optical nonlinearity emerge in the directions of $2k_2$-k_1 and $2k_1$-k_2.[15,16] The diffraction efficiency, the ratio of the signal intensity to the probe beam (I_s/I_p), should depend on the square of pump beam intensity. The diffraction ef-

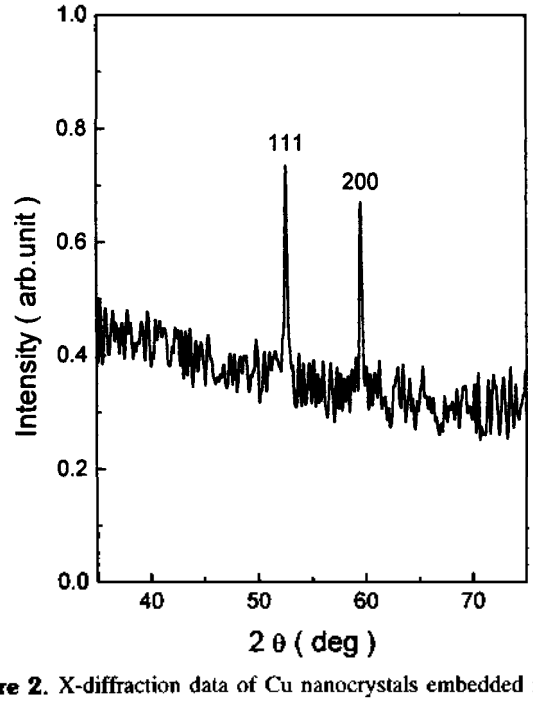

Figure 2. X-diffraction data of Cu nanocrystals embedded in silicate glass.

Figure 3. High resolution TEM micrograph of ion-implanted Cu-SiO_2 thin films heat-treated at 700 °C.

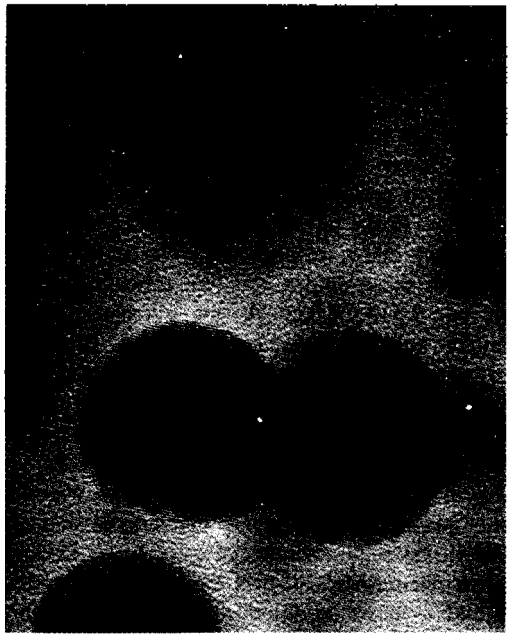

Figure 4. TEM micrograph showing the interference pattern of Cu nanocrystals embedded in silica glass.

ficiency was plotted in Figure 5 as a function of the peak intensity of the probe beam in the logarithm scale. The diffraction efficiency is fairly linear and the slope is 1.7, elucidating approximate square dependence.

For two beam DFWM, the $\chi^{(3)}$ value can be calculated from the following equation:[15,16]

$$\chi^{(3)} = \frac{n^2 c}{2^5 \pi^3} \lambda \frac{\alpha}{(1-T)T^{1/2}} \frac{\eta^{1/2}}{I_p} \tag{2}$$

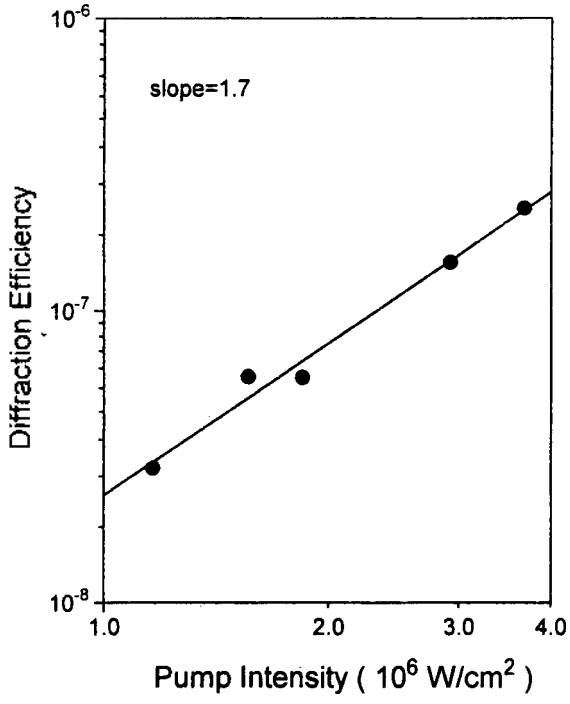

Figure 5. Diffraction efficiency of Cu-SiO_2 thin films as a function of laser pump intensity.

where n is the linear refractive index, c the light speed in vacuum, I_p the pump intensity, the linear absorption coefficient, and η the diffraction efficiency. The transmittance T is given by $\exp(-\alpha l)$ in which l is the sample thickness.

The calculated $\chi^{(3)}$ values as a function of laser wavelength in the 540-570 nm region are in the range of (0.4-1.1) $\times 10^{-8}$ esu with the maximum value at 560 nm. Due to laser fluctuation ($\pm$20%) and tunability of the dye laser, it was difficult to obtain the dispersion of $\chi^{(3)}$ in the whole surface plasmon absorption region. The $\chi^{(3)}$ values of Cu-SiO_2 thin films have been reported as 10^{-8}-10^{-10} esu. Our value of 8.5×10^{-9} esu on average lies in the previously reported values. However, for comparison of our measured value with other reported data, it is necessary to use $\chi_m^{(3)}$, the nonlinear optical coefficient of metal itself, rather than the obtained value of the thin-film sample. This is because the third order nonlinear optical coefficient of nanoparticles embedded in dielectric media depends on nanocrystal contents (volume fraction). $\chi_m^{(3)}$ is related to $\chi^{(3)}$ by

$$\chi_m^{(3)} = \frac{\chi^{(3)}}{p\,|f_i(\omega)|^2 f_i(\omega)^2} \tag{3}$$

where p is the volume fraction of metal particles in composite materials and $f_i(\omega)$ is the local field factor. According to the Maxwell-Garnett theory, the local field factor is the ratio of the local electric field inside the particle to the applied field:[17]

$$f_i(\omega) = \frac{E_i}{E_o} = \frac{3\varepsilon_d(\omega)}{\varepsilon_m(\omega) + 2\varepsilon_d(\omega)} \tag{4}$$

ε_m is the complex value of the dielectric constant of the metal particle. For bulk Cu crystals, the dielctric constant can be obtained from Ref. 18. The local field factor is a complex number, because the dielectric constant is complex. However, we measure the absolute value of $\chi^{(3)}$ by DFWM, so Eq. (4) can be rewritten as (3) $|\chi(3)|=p|f_i(\omega)|^4\chi_m^{(3)}|$. In the vicinity of the surface plasmon resonance the absorption coefficient is related to the local field factor and the imaginary part of the dielectric constant of metal particles by[6]

$$\alpha = p(\omega/nc)\,|f_i(\omega)|^2 \varepsilon_m'' \tag{5}$$

From Eq. (3)-(5), the $\chi_m^{(3)}$ value was calculated as 5.6×10^{-8} esu. Yang *et al.* observed dependence of $\chi_m^{(3)}$ value on Cu nanocrystal size.[13] For nanocrystal size of 13 nm which is comparable to ours, they obtained $\chi_m^{(3)}$ value of 5.3×10^{-9} esu. Therefore, our value of 5.6×10^{-8} esu is about one order larger than their results. Recently, Nakamura and coworkers measured $\chi_m^{(3)}$ of Cu and Ag nanocrystals both of which were prepared by high temperature glass melting technique.[19] They observed huge difference between $\chi_m^{(3)}$ of Cu nanocrystals and that of Ag nanocrystals: They explained high optical nonlinearity of Cu nanocrystals in terms of resonant enhancement due to d-sp transition in copper in surface plasmon absorption region, which do not appear in silver. This indicates that hot electrons generated by interband transition also contribute to the third-order optical nonlinearity. In addition to this, it has been known that local heating is expected to contribute to optical nonlinearity.[20] We think the difference between Yang *et al.*'s results and ours both of which were prepared by the similar procedure arises from

thermal effects, because our DFWM experiment was carried out using a nanosecond pulse (8 ns), while they used much shorter pulse (35 ps). Therefore, the importance of our results is in verifying that thermal effects are one of very important factors affecting third-order optical nonlinearity of metal nanoparticles.

Conclusion

Copper nanoparticles in silica glass were prepared by ion-implantation and high temperature heat-treatment. Their structure was characterized by X-ray and high resolution TEM. Using DFWM, third-order nonlinear optical coefficients of copper nanoparticles were measured in the surface plasmon absorption region (540-570 nm) as $(0.4\text{-}1.1)\times 10^{-8}$ esu. The large thermo-optic nonlinearity can be explained by the interband transition, surface plasmon resonance, and hot electron effects.

Acknowledgment. This work has been financially supported by Korea Ministry of Education (BSRI-96-3427). The authors thank Prof. Y. S. Choi for helping the DFWM experiment.

References

1. Kreibig, U.; Vollmer, M. *Optical Properties of Metal Clusters*; Springer: Berlin, 1995.
2. Kreibig, U.; Genzel, L. *Surf. Sci.* **1985**, *156*, 678.
3. Creighton, J. A.; Eadon, D. G. *J. Chem. Soc., Faraday Trans.* **1991**, *87*, 3881.
4. Heilweil, E. J.; Hochstrasser, R. M. *J. Chem. Phys.* **1985**, *82*, 4762.
5. Dutton, T.; Vanwonterghem, B.; Saltiel, S.; Chestnoy, N. V.; Renzepis, P. M.; Shen, T. P.; Rogovin, D. *J. Phys. Chem.* **1990**, *94*, 1100.
6. Henglein, A. *J. Phys. Chem.* **1993**, *97*, 5457.
7. Hache, F.; Ricard, D.; Flyzanis, C.; Kreibig, U. *Appl. Phys. A* **1988**, *47*, 347.
8. Kozuka, H.; Sakka, S. *Chem. Mater.* **1993**, *5*, 222.
9. Matsuoka, J.; Mizutani, R.; Kaneko, S.; Nasu, H.; Kamiya, K.; Kadono, K.; Sakaguchi, T.; Miya, M. *J. Cer. Soc. Japan* **1993**, *101*, 53.
10. Gacoin, T.; Chaput, F.; Boilot, J. P.; Jaskierowicz, G. *Chem. Mater.* **1993**, *5*, 1150.
11. Lee, M.; Kim, T. S.; Choi, Y. S. *J. Non-Crystalline Solids* **1997**, *211*, 143.
12. Magruder III, R. H.; Zuhr, R. A.; Weeks, R. A. *Nucl. Instr. Methods* **1991**, *B59/60*, 1308.
13. Yang, L.; Becker, K.; Smith, F. M.; Magruder III, R. H.; Haglund, Jr., R. F.; Yang, L.; Dorsinville, R.; Alfano, R. R.; Zuhr, R. A. *J. Opt. Soc. Am. B* **1994**, *11*, 457.
14. Arnold, G. W. *J. Appl. Phys.* **1975**, *46*, 4466.
15. Nakamura, A.; Tokizaki, T.; Akiyama, H.; Kataoka, T. *J. Lumin.* **1992**, *53*, 105.
16. Lee, M. *Bull. Korean Chem. Soc.* **1995**, *16*, 126.
17. Perenboom, J. A. A.; Wyder, P. F. *Phys. Rep.* **1981**, *78*, 173.
18. Johnson, P. B.; Christy, R. W. *Phys. Rev. B* **1972**, *6*, 4370.
19. Uchida, K.; Kaneko, S.; Omi, S.; Hata, C.; Tanji, H.; Asahara, Y.; Ikushima, A.; Tokizaki, T.; Nakamura, A. *J. Opt. Soc. Am. B* **1994**, *11*, 1236.
20. Cui, Y.; Zhaox, M.; He, G. S.; Prasad, P. N. *J. Phys. Chem.* **1991**, *95*, 6842.